Infrared stealthy surfaces: Why TES and THEMIS may miss some substantial mineral deposits on Mars and implications for remote sensing of planetary surfaces

Laurel E. Kirkland[1,2], Kenneth C. Herr[2], Paul M. Adams[2]

[1]Lunar and Planetary Institute, 3600 Bay Area Blvd., Houston, TX 77058
[2]The Aerospace Corp., P.O. Box 92957, Los Angeles, CA 90009

Correspondence address:
Laurel Kirkland
Lunar and Planetary Institute
3600 Bay Area Blvd., Houston, TX 77058
email: kirkland@lpi.usra.edu
phone: 281-486-2112
fax: 281-486-2162

Abstract. Infrared spectral observations have yielded many important insights into the nature of Mars. However, spectral effects tied to surface roughness and particle size can make mineral deposits substantially more difficult to detect and identify than is generally known, including for current investigations. The effects hold for Mars and other planets, but here we focus on the impact on the exploration of Mars. Laboratory spectra of pure, smooth-surfaced minerals have previously been used to conclude that the 1996 Global Surveyor Thermal Emission Spectrometer (TES) and the 2001 Mars Odyssey Thermal Emission Imaging System (THEMIS) will detect a mineral deposit that covers ~10% of a pixel. Those laboratory spectra have formed the foundation for modeling and interpretations of TES/THEMIS data and for development of the 2003 Mars rover Mini-TES. Here, for the first time, we compare TES/THEMIS foundation data to laboratory, field, and unique airborne spectra of rough surfaces. We demonstrate that substantial, well-crystalline, regional mineral deposits, including rock outcrops, can be 100% exposed and remain undetected at the sensitivity of TES/THEMIS. We then detail the physics, which apply to all geologic materials. Previous studies have demonstrated the complicating physical effects for solids vs. particulates for a range of minerals, including oxides, sulfates, carbonates, and each of the seven silicate classes. We identify three cases of spectral behavior that can impact interpretations: In Case 1, physical effects cause a target to be undetectable by a given infrared instrument ("infrared stealthy"). In Case 2, variations in spectral contrast mimic abundance variations, which confounds abundance mapping. In Case 3, alteration of the spectral band shape impacts compositional interpretations. Optically smooth materials will be well-represented in TES/THEMIS/Mini-TES identifications. Conversely, if a material forms an optically rough surface or sufficiently small particles on Mars, then it will be comparatively underrepresented or missed. Surface roughness occurs on three broad scales, and roughness at the grain scale can be a primary variable in whether a mineral is detectable. Non-detection of certain key minerals (e.g., carbonates) can significantly impact geologic and climatic interpretations and landing site selection. The TES/THEMIS detection threshold may be 10% coverage based on specific laboratory samples, but for field measurements, that prediction represents an idealized lower bound. Interpretations built on non-detection should be revisited after defining the uncertainties in detection capabilities for specific instruments as applied to expected mineral surface textures on Mars, including at the grain scale. The impact on future measurement strategies (including Mini-TES) should also be assessed.

1. Background

Mineral identification and mapping are fundamental components in the exploration of Mars and other planets. For example, the presence or absence of carbonate on Mars is considered a key indicator of past climatic and hydrologic activity [*Carr*, 1996; *Carr and Head*, 2003]. If Mars had a denser CO_2 atmosphere in its past and liquid water on its surface, then large deposits of carbonate materials likely would have formed [*Pollack et al*., 1987]. Similarly, it is expected that large hydrothermal systems on Mars would be marked by carbonate deposits [*Farmer and Des Marais*, 1999]. These areas would be prime candidates for astrobiology landing sites [*Farmer and Des Marais*, 1999]. Thus carbonate detection would influence landing site selection [*Carr et al*., 1994; *Farmer and Des Marais*, 1999], but in the absence of detection, site selection shifts to other targets.

Under specific conditions, carbonates will exhibit distinct bands centered near 6.5, 11.2, and 33 μm. *Blaney and McCord* [1989] and *Roush et al*. [1993] reviewed proposed carbonate detections on Mars prior to TES/THEMIS. The reported detections have not widely been perceived as conclusive. It was intended that two recent orbiter-based infrared instruments would conclusively resolve whether carbonates are present on Mars (the 1996 Mars Global Surveyor TES [*Christensen et al*., 2001] and the 2001 Mars Odyssey THEMIS [*Christensen et al*., 1999]). However, conclusive detections have not been forthcoming. *Christensen et al*. [2001] concluded that TES detected no carbonate deposits at the 10% level. *Bandfield and Smith* [2003] concluded that TES detected no carbonate bands in selected dark regions to the 5% level, including using spectra measured of <45 μm particles. Complexities in atmospheric retrievals have delayed an examination of the 6.5 μm region in TES spectra, particularly for bright regions. *Bandfield et al*. [2003] recently proposed detection of a 6.5 μm band in TES data that they attribute to carbonate in the Martian surface dust. However, the interpretation remains inconclusive without a concurrent detection of the 11.2 and 33 μm carbonate bands. No definitive carbonate bands have been reported in THEMIS data. The 2003 rover Mini-TES will measure spectra comparable to TES, and Mini-TES is similarly intended to resolve what minerals are present [*Christensen et al*. 2000a].

The lack of definitive detection of carbonate deposits has been widely interpreted as significantly constraining the presence of a massive early greenhouse atmosphere and large bodies of liquid water (oceans or seas) [*Carr*, 1996; *Carr and Head*, 2003]. The assertion that both TES and THEMIS will identify minerals at the 10% coverage level [*Christensen et al*., 2001; *Christensen et al*., 1999] is broadly perceived as significantly tightening the constraint on the possible presence of carbonate. This 10% threshold estimate is based on spectra of a specific type of laboratory sample: pure minerals, hand samples or sieved to large particle sizes, washed, and smooth-surfaced at multiple scales [*Christensen et al*., 2000b].

Current interpretations of the lack of clear carbonate detections include: this material (and thus abundant water) was never there [*Christensen et al*., 2001]; it is buried or dust-covered [*McKay and Neddel*, 1988; *Clark*, 1999, *Christensen et al*., 2001]; it is altered by UV radiation or subsequent chemical reactions [*Mukhin*, 1996; *Clark*, 1999], although this explanation is debated [*Fonti et al*., 2001]; or it occurs exclusively as a dispersed contaminant or in small deposits (exposed over less than one-tenth of the TES ~3 km x 5 km or THEMIS 100 m x 100 m field of view) [*Farmer and Des Marais*, 1999; *Christensen et al*., 2001].

The "White Rock" deposit in Pollack Crater has been proposed as a possible lacustrine deposit [*Williams and Zimbelman*, 1994]. However, that interpretation was discounted because TES did not detect any mineral signature there [*Ruff et al*., 2001]. On the other hand, in other regions TES has detected a signature consistent with coarse hematite [*Lane et al*., 1999; *Christensen et al*., 2000c] or a hematite coating [*Kirkland et al*., 2001a; *Kirkland et al*., 2003a]. The importance and rarity of clear detections of a potentially interesting mineral led to the selection of that site for a 2003 rover mission. Thus high confidence in non-detection has altered interpretations of the geologic and hydrologic history of Mars and of specific deposits. It also impacts landing site selection because sites that are perceived to lack interesting minerals are considered of lesser importance.

Although widely unrecognized, another possible explanation for the non-detection of mineral deposits is that they may have surface textures

that make them difficult to identify spectroscopically (i.e., they may have stealthy infrared properties). Surface roughness is a common, effective, and longstanding means to construct blackbody-like surfaces that infrared instruments cannot identify [*Williams*, 1961; *LaRocca*, 1971; *Kirkland et al*., 2002a]. A blackbody has an emissivity of one and a featureless spectrum, which thus has no spectroscopic compositional information (an infrared stealthy surface). Thus it is well known that multiple surface reflections make a target less detectable, and surface roughness causes multiple surface reflections in opaque geologic materials.

Salisbury et al. [1991] illustrate the spectral contrast reduction in smooth vs. particulate surfaces for a wide range of geologic materials, including silicates, sulfates, and carbonates. The contrast reduction is further illustrated and explained in *Salisbury* [1993]. However, variations in surface texture extend well past particulate vs. solid surfaces. A wide variety of surface textures occurs in nature, and the texture is commonly influenced by formation and weathering processes. Weathering processes may couple with the grain size, chemical composition, and microstructure to cause further variety. Coatings can also contribute additional textural diversity.

Thus texture can impact the spectral signature of all geologic classes, and a wide range of textures occurs in nature. Those points make it critical to (1) understand and convey the impact of surface texture on spectral variation and (2) combine an understanding of the physics with a repeatable method to define detection limits for an instrument and intended target characteristics. Here we summarize a simple method and use it to illustrate the importance of spectral behavior on the detectability of a mineral deposit. We then demonstrate the causes of variations in spectral contrast, the importance to mineral detection, and the impact on interpretations of Mars.

2. Mineral Detection

The ability to detect a mineral varies with material composition, surface texture and particle size, and sensitivity of the instrument. Thus a well-defined geologic interpretation first requires defining both the spectral properties of the proposed target material and the instrument capabilities.

Band detection limit. Current TES interpretations use laboratory spectral signatures (foundation studies) of pure minerals that are hand samples or crushed, sieved to large particle sizes (710–1000 μm), and washed [*Christensen et al*., 2000b]. Figure 1a shows an example calcite spectrum ("C8"), and Figure 1b focuses on the 11 μm region in more detail. This spectrum exhibits an 11 μm band contrast (*d*) of ~40%. A spectrum with this contrast was selected to match the contrast of the *Christensen et al*. [2001] Plate 11 carbonate spectrum, which *Christensen et al*. used to support their conclusion that TES has not detected carbonates on Mars to the 10% level. When comparing the data, note that *Christensen et al*. [2001] scaled their Plate 11 spectrum to simulate 10% surface coverage (i.e., 40% contrast for 100% coverage is 4% contrast at 10% coverage). It is important to determine whether a comparison using a spectrum that exhibits different spectral contrast would lead to a different detection limit conclusion than 10%.

The minimum fractional exposure by a target material (f_{min}) required for detection is [*Kirkland et al*., 2001b]:

$$f_{\min} = \frac{DL}{d} \qquad (1)$$

where *d* is the band contrast exhibited by the target (e.g., Fig. 1 illustrates $d \cong 0.4$). *Lyon* [1964] and *Clark and Roush* [1984] also detail the definition of band contrast (band depth). *DL* is the band detection limit, which is the minimum observed band depth required to accept as a detection for a given band width and center.

Equation 1 shows that the minimum fractional coverage by a mineral deposit required for detection increases as the band contrast (*d*) exhibited by the material decreases, i.e. as the band "flattens". If a laboratory spectrum exhibits absorption bands that are not observed in TES or THEMIS data, then currently it is concluded that the mineral is not present for ~10% coverage of a TES or THEMIS pixel [*Christensen et al*., 2001; *Christensen et al*., 1999], i.e. the published $f_{\min}$ is ~10%.

It is critical to understand that the strongest spectral band in a laboratory spectrum is not necessarily the most detectable by a given flight instrument [*Kirkland et al*., 2001b]. For example, the rapidly decreasing signal-to-noise ratio toward

shorter wavelength in TES data makes the carbonate 11 µm band in the Fig. 1 spectra more detectable than the 6.5 µm carbonate band by TES, even though the 11 µm band is narrower and weaker in laboratory spectra (Fig.1a) [*Kirkland et al.*, 2001b]. This situation occurs because the instrument signal-to-noise ratio varies with wavelength, so the minimum band depth required for detection (*DL*) also varies with wavelength.

Quantitative statements of non-detection require inclusion of (1) the band that is most detectable by the given instrument; (2) the band depth that it is assumed the target will exhibit (*d*); and (3) the minimum band depth detectable by the instrument (*DL*) at the wavelength of interest.

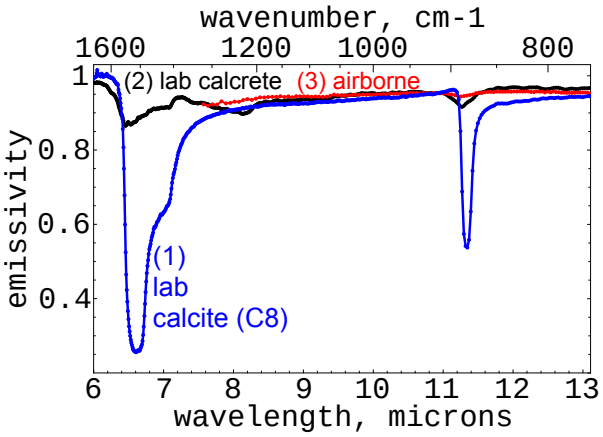

Figure 1a: Spectral contrast variation. (1) The lower, blue trace (sample "C8") is a laboratory spectrum of a calcite hand sample [*Christensen et al.*, 2000b, 2001]. The upper spectra are (2) a laboratory spectrum of an intensely lithified hand sample of calcrete (sample "mm4bhr") and (3) an airborne spectrum of a region covered with calcrete boulders. This illustrates the reduced spectral contrast that can make even regional outcrops undetectable. In addition, when examining laboratory spectra, it is important to understand that the strongest band in a laboratory spectrum is not necessarily the most detectable by a given flight instrument. For example, the rapidly decreasing signal-to-noise ratio of TES at shorter wavelengths makes the weaker, narrower 11 µm band more detectable by TES than the 6.5 µm band [*Kirkland et al.*, 2001b]. The airborne and C8 spectra are in apparent emissivity. The laboratory calcrete spectrum is in true emissivity (one minus hemispherical reflectance). For clarity the airborne spectrum is offset -0.042 to match the calcrete emissivity at 11.6 µm.

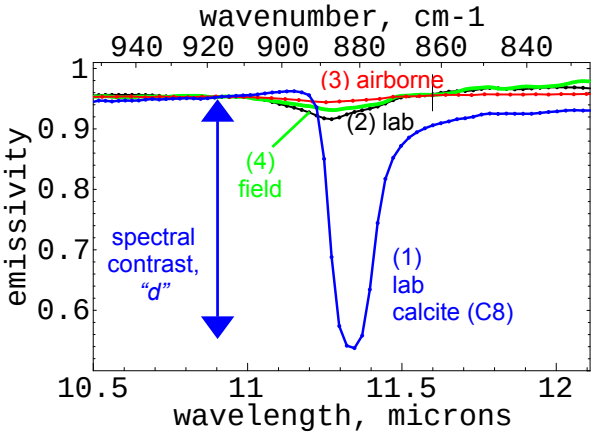

Figure 1b: Spectral contrast variation. This shows addition detail of the 11 µm region for the three spectra in Figure 1a, plus (4) a field spectrometer signature measured of the same target region as the airborne spectrum, shown in apparent emissivity. The left, vertical arrow illustrates the approximate spectral contrast (*d*) of the C8 calcite spectrum. For clarity the field and airborne spectra are offset to match the true emissivity of the laboratory spectrum at 11.6 µm (vertical reference line), with offsets of airborne -0.042 and field -0.0045.

3. Airborne, Field, Laboratory Data

Laboratory data. All laboratory spectra shown here were measured from hand samples; none are of particulates or coatings. That approach was selected to (1) examine the variety of spectral behavior that can occur in lithified material, and (2) provide the most direct comparison to the airborne and field data, which similarly targeted regions with near 100% coverage by rocks. The laboratory reflectance measurements were made at The Aerospace Corporation and used a Nicolet Magna 550 Fourier transform spectrometer. Biconical reflectance measurements (2.5–200 µm) used a "praying mantis" diffuse attachment. Hemispherical reflectance measurements (2.5–25 µm) used a Labsphere 3-inch diameter integrating sphere (approximately 5 mm diameter spot size) to determine absolute emissivity via Kirchhoff's Law as derived from conservation of energy (emissivity = 1- reflectance) [*Nicodemus*, 1965; *Judd*, 1967; *Korb et al.*, 1999]. We examined the upward facing weathered surfaces (as marked in the field) to better correlate laboratory

and field spectra. *Kirkland et al*. [2002a] further detail the laboratory instrumentation. The publicly available TES spectral library data are in apparent emissivity [*Christensen et al*. 2000b].

Airborne and field data. The airborne data were measured by the SEBASS imaging spectrometer [*Hackwell et al*., 1996; *Kirkland et al*., 2001b; *Kirkland et al*., 2002a]. SEBASS is the Spatially Enhanced Broadband Array Spectrograph System. It is owned by The Aerospace Corporation, a non-profit Federally Funded Research and Development Center. SEBASS is accessible for research, and it covers 7.6–13.5 μm in 128 channels. Atmospheric water vapor and CO_2 limit terrestrial thermal infrared airborne studies of the surface to that range. The data used here have a spatial resolution of 2 m × 2 m, with images 128 pixels wide and 4000 pixels long. SEBASS measures with the highest signal-to-noise ratio of any airborne thermal infrared imaging spectrometer. The field spectra were measured by a van-mounted Brunswick Model 21 interferometer spectrometer, covering 6.68–14.28 μm, with a ~0.3 m × 0.3 m pixel size, and 4 cm^{-1} apodized spectral resolution. *Kirkland et al*. [2002a, 2002b] further detail the instruments and data processing.

The airborne and field data are processed to apparent emissivity, as is also done for TES and THEMIS data of Mars [e.g., *Hanel et al*., 1992; *Smith et al*., 2000] and the TES team public spectral library [*Christensen et al*. 2000b]. True emissivity is the measured radiance divided by the Planck blackbody radiance at the true sample kinetic temperature. This change of units from radiance to emissivity is termed a conversion. When the kinetic temperature is not measured by an independent means, it must be estimated. When the kinetic temperature is estimated, then the converted result is termed apparent emissivity [*Ginsburg et al*., 1960; *Conel*, 1969]. One method to convert remote sensing data is by using the highest brightness temperature as the estimated kinetic temperature (e.g., *Kahle and Alley*, 1992; *Hook et al*., 1999). This is the method that has been used in most geologic studies of Mars that use data from spacecraft-carried instruments [*Hanel et al*., 1992; *Smith et al*., 2000], for the airborne and field data presented here [*Kirkland et al*., 2001b, *Kirkland et al*., 2002a], and also in some laboratory studies that measure in emission rather than reflectance [e.g., *Conel*, 1969; *Christensen et al*. 2000b].

Calcrete and limestone samples. The laboratory, field, and airborne measurements included samples of indurated calcite (calcrete) from Mormon Mesa, Nevada [*Kirkland et al*., 2002a]. The calcrete is intensely lithified and requires strong hammer blows to break it. The calcrete source is a distinct, regional geologic unit, not a coating (*Gardner*, 1968; *Gardner*, 1972). Its density is near that of calcite, with an average density of 2.62 g/cm^3 for the calcrete [*Gardner*, 1972] vs. 2.72 g/cm^3 for a calcite crystal and 2.65 g/cm^3 for a quartz crystal [*Klein and Hurlbut*, 1993]. In the region with airborne data, areas predominantly or fully covered by calcrete had calcrete particle sizes ranging from several centimeters to boulders. The calcrete is ~90% calcite and ~10% quartz. X-ray diffraction (XRD) was used to identify the major phases present. The grains are well-crystalline. Crystalline is defined as a material that has regular molecular structure [*Bates and Jackson*, 1983]. The limestone hand sample is also from Mormon Mesa, and is ~99% carbonate [*Kirkland et al*., 2002a]. Multiple samples were tested, and for all samples, carbonate contents were determined by gravimetric acid digestion. Sample surfaces were examined by scanning electron microscopy (SEM) and chemically characterized by energy dispersive X-ray spectroscopy (EDXS). Cross-section SEM images, EDXS measurements, and the spectral signature over the 2.5–50 μm range give no indication of a coating [*Kirkland et al*., 2002a]. In addition to EDXS, the spectral shape in the 14 μm range can be used to determine whether the calcrete has significant Mg substitution [e.g., *Huang and Kerr*, 1960; *Adler and Kerr*, 1963; *White*, 1974; *Lane and Christensen*, 1997], and the spectra are consistent with calcite.

Comparison of laboratory, field, and airborne data. Figure 1a and 1b illustrate that laboratory, field, and airborne spectral contrasts can be significantly attenuated relative to the foundation spectra used to interpret TES and THEMIS data and to predict the 10% detection limit. The SEBASS and field studies illustrate that this can occur for massive geologic materials in regional deposits.

Figure 1b shows a calcite spectrum from the TES public spectral library [*Christensen et al*. 2000b], spectra measured by the field and air-

borne spectrometers of regions with near 100% coverage by lithified calcite (calcrete), and a laboratory spectrum of calcrete [*Kirkland et al*., 2002a]. Scattering effects contribute to the band center offsets [*Salisbury et al*., 1991]. *Gardner* [1968] and *Gardner* [1972] detail the geology of the Mormon Mesa region. *Kirkland et al.* [2002a] detail the associated SEBASS and field spectrometer study, and include pictures of the calcrete, additional references, and a SEBASS site image.

4. Causes of Reduced Spectral Contrast

Surface properties unrelated to composition attenuate spectral contrast. These are: (1) roughness that causes multiple surface reflections in opaque material, and (2) particle size and texture on a scale that causes volume absorption [*Williams*, 1961; *Lyon*, 1964; *Van Tassel and Salisbury*, 1964; *Aronson et al*., 1966; *Hovis and Callahan*, 1966; *Aronson et al*., 1967; *Goetz*, 1968; *Hunt and Vincent*, 1968; *Vincent and Hunt*, 1968; *Conel*, 1969; *Hunt and Logan*, 1972; *Hunt*, 1976; *LaRocca*, 1978; *Hapke*, 1983; *Salisbury et al*., 1987; *Salisbury et al*., 1991; *Hanel et al*., 1992; *Salisbury and Wald*, 1992; *Fraden*, 1993; *Kirkland et al*., 2001b; *Kirkland et al*., 2002a, *Le Bras and Erard*, 2003].

Surface roughness. Surface roughness is a common means to improve a blackbody target because it increases the overall emissivity and decreases the spectral contrast [*Williams*, 1961; *LaRocca*, 1978]. The concurrent increase in emissivity and decrease in spectral contrast is called a hohlraum or cavity effect. An example is the TES onboard blackbody calibration target, which uses 45 degree parallel grooves that are 1.5 mm deep in combination with a high emissivity paint [*Christensen et al*., 2001].

Roughness that causes multiple surface reflections includes the grain texture, grooves, vesicles, the gaps between rocks in a mound, interstices between grains, and pits and cracks in rocks. Multiple reflection effects are observed for roughness to at least ~one-fifth the wavelength [*Siegel and Howell*, 1968], and in the other direction, macroroughness (e.g., a mound of boulders) will also cause multiple reflections.

Figure 2 illustrates the decrease in spectral contrast with multiple reflections. The increase in effective emissivity (ε_e) with the number of reflections (ξ) from a surface (e.g., a mineral facet) with true emissivity ε is given by [*Aronson et al*., 1967; *Williams and Becklund*, 1984; *Fraden*, 1993]:

$$\varepsilon_e = 1 - (1 - \varepsilon)^{(\xi+1)} \qquad (2)$$

Broadly, a cavity effect increases as the ratio of the cavity depth to entrance width increases [*Williams and Becklund*, 1984]. An examination of blackbody behavior has been a longstanding area of research due to the importance of blackbody simulators in a range of applications. However, in practice, calculating the number and distribution of multiple reflections (and thus the total, quantified cavity effect) has proven a complex problem, even for simple shapes [e.g., *Williams*, 1961; *LaRocca*, 1978; *Bartell*, 1981; *Bedford et al.*, 1985]. The cavity effect varies with the cavity shape, cavity area, entrance aperture area, the material emissivity, and whether the surface reflects diffusely or specularly [*Williams*, 1961; *LaRocca*, 1978; *Bartell*, 1981; *Williams and Becklund*, 1984; *Bedford et al.*, 1985]. Nonetheless, the trend is long known and clear: multiple surface reflections decrease the spectral contrast and increase the emissivity.

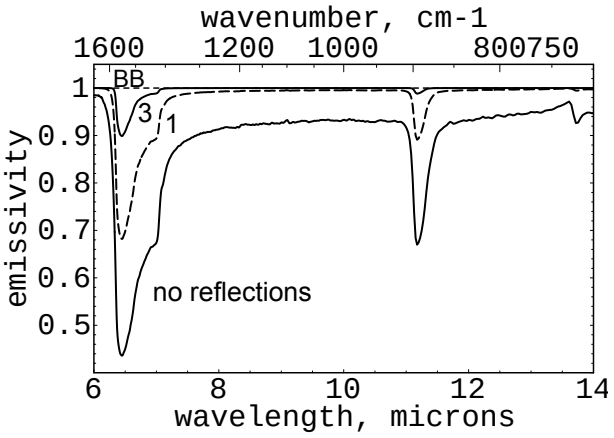

Figure 2: Cavity effect in limestone. The lower solid trace shows the measured spectrum of a fresh surface of a limestone hand sample. The upper traces simulate one and three reflections using Equation 2. Note the increasing continuum emissivity and the contrast reduction of all bands. The dashed line "BB" illustrates an ideal blackbody spectrum. Sample mmlssep00, shown as emissivity equals one minus hemispherical reflectance.

Surface reflection vs. volume absorption. The presence of partially transmissive (optically thin) material can also decrease the spectral contrast. A strong absorption band causes high opacity, so incident radiance cannot penetrate the surface more than a fraction of the wavelength [*Hecht*, 1987]. Thus in regions of strong bands, little incident radiance is transmitted or absorbed, so most is reflected. This reflection from the surface is termed "surface scattering." Scattering is when radiance is deflected in the same medium from the original direction of propagation [*Haertel*, 1978]. The resulting mirror-like surface produces reflectance peaks called "reststrahlen bands" [*Hunt and Vincent*, 1968; *Conel*, 1969; *Hunt and Logan*, 1972; *Salisbury et al*., 1987; *Salisbury and Wald*, 1992; *Fabbri et al*., 2001; *Kirkland et al*., 2002a]. In the case of emission, the surface of a body reflects radiance inward at reststrahlen bands [*Planck*, 1914], causing an emissivity reduction (emissivity trough). The Figure 3 solid surface spectrum illustrates this in the carbonate 6.5 and 11 μm absorption troughs.

On the other hand, volume absorption occurs when some radiance transits completely through the material [*Lyon*, 1964; *Aronson et al*., 1966; *Aronson et al*., 1967; *Vincent and Hunt*, 1968; *Conel*, 1969; *Hunt and Logan*, 1972; *Salisbury et al*., 1987; *Elachi*, 1987; *Salisbury et al*., 1991; *Salisbury and Wald*, 1992; *Mustard and Hays*, 1997; *Fabbri et al*., 2001; *Kirkland et al*., 2002a]. When radiance survives passage through a volume of a grain and is then reflected by a grain boundary to the observer, it is termed "volume scattering." Thus volume scattering refers to reflections that occur after the radiance transits through a volume of the material, and surface scattering refers to reflections that occur without transiting through the material. Volume absorption can occur by direct transmission or after volume scattering.

Volume absorption increases as particles become small enough to become optically thin (partially transmissive), or when they have optically thin edges. When volume absorption dominates, the reststrahlen band shapes appear as emission peaks rather than troughs, and they are slightly offset to longer wavelength (Fig. 3) [*Hunt*, 1965; *Salisbury et al*., 1991]. Thus volume absorption can attenuate spectral contrast because the trend counters that of surface reflectance (Fig. 3).

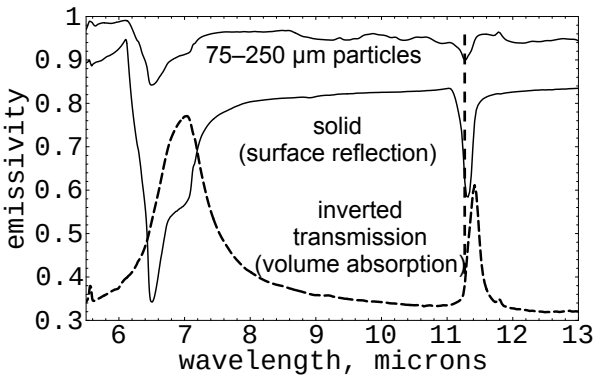

Figure 3: Volume absorption vs. surface reflection for calcite. These spectra are of calcite (sample "calcite.1" from *Salisbury et al*. [1991]). The transmission spectrum is of <2 μm particles, which are optically thin, so volume absorption dominates. The transmission spectrum is inverted to plot in emissivity (emissivity = one minus transmission, Kirchhoff's Law from conservation of energy [*Nicodemus*, 1965; *Hunt*, 1965, *Williams and Becklund*, 1984]), offset and scaled for clarity using 0.82-(transmission/100). For the solid sample, surface reflection dominates. The coarse particle (75–250 μm) spectrum exhibits some volume absorption, evident in the altered band shapes. Multiple reflections from gaps between the particles also reduce the spectral contrast and increase the continuum emissivity. The transmission spectrum illustrates the typical offset of band centers toward longer wavelength relative to the solid surface spectrum. This causes the shift in the coarse particle 11 μm band center (marked by the vertical dashed line) as volume absorption alters the long wavelength side of the 11 μm band. The solid and coarse particles were measured in biconical reflectance [*Salisbury et al*., 1991] and converted to approximate emissivity using one minus reflectance. Biconical measurements accurately show the spectral shape, but not the absolute emissivity [*Salisbury et al*., 1991].

Demonstration of the effects. Figure 4 shows the first demonstration of altered spectral contrast and shapes that are caused by changes made only to the surface texture of the same geologic hand sample. It is critical to recognize that texture alone can cause the observed spectral variations, and that the variety can occur both in particulate [*Salisbury et al*., 1991] and consolidated targets.

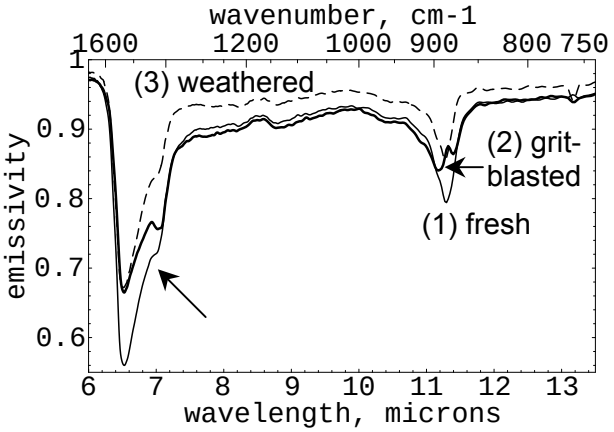

Figure 4a: Spectral variations caused by texture in a limestone hand sample. Relative to (1) the fresh limestone surface, the (2) grit-blasted surface shows altered spectral band shape (arrows) and slightly lower continuum emissivity, consistent with volume scattering. The (3) weathered surface has higher continuum emissivity, reduced spectral contrast, and no clear alteration of the band shapes, consistent with a cavity effect. Sample 4-12-C, in emissivity (one - hemispherical reflectance).

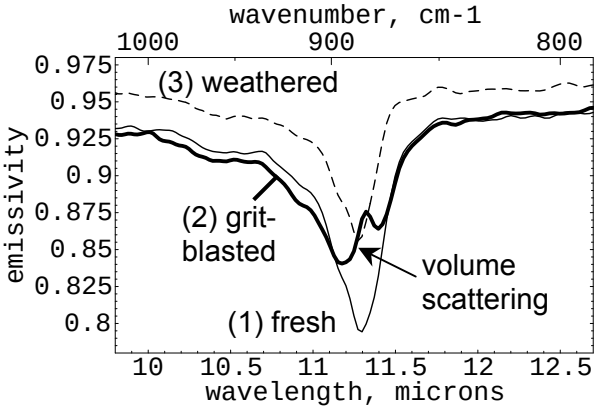

Figure 4b: Close-up of 11.2 µm region for the limestone hand sample. This illustrates additional details of 11.2 µm band behavior shown in Fig. 4a. Note the (3) weathered surface exhibits reduced spectral contrast and higher emissivity relative to the (1) fresh surface, but has the same band shape as the fresh sample. In the (2) grit-blasted spectrum, volume scattering alters the band shape (right arrow) and shifts the band center. A change in the band shape can affect compositional modeling. A change in the band center can affect interpretations that utilize the band center as a measure of composition.

Figure 4a shows the following spectra measured of a limestone hand sample from Mormon Mesa: (1) the exposed, weathered surface; (2) a fresh surface; and (3) a surface that was saw cut, ground with a coarse grinding wheel, grit blasted with coarse Al_2O_3, and then cleaned in an ultrasonic cleaner. XRD measurements show that the grit-blasting did not cause any alteration to aragonite. The weathered limestone spectrum has reduced spectral contrast and a higher continuum emissivity relative to the fresh surface, but the band shapes are not altered. Both the continuum emissivity and band shape are consistent with a cavity effect. The grit-blasted spectrum shows volume scattering in the lower continuum emissivity and altered 6.5 and 11.2 µm band shapes. This evidence of volume scattering indicates that the grit blasting caused micro-fracturing of the surface. Figure 4b illustrates in more detail the 11.2 µm band.

Figure 5a shows an SEM cross-section image of a freshly broken limestone surface. The relatively smooth surface gives few opportunities for multiple reflections. The lighter material is calcite, and the darker material is dolomite. Figure 5b shows the weathered limestone surface. The pits will cause a cavity effect. Figure 5c shows the grit-blasted limestone surface. The thin, fractured material at the surface causes the volume scattering evident in Figure 4. However, the relatively smooth surface gives less opportunity for multiple surface reflections.

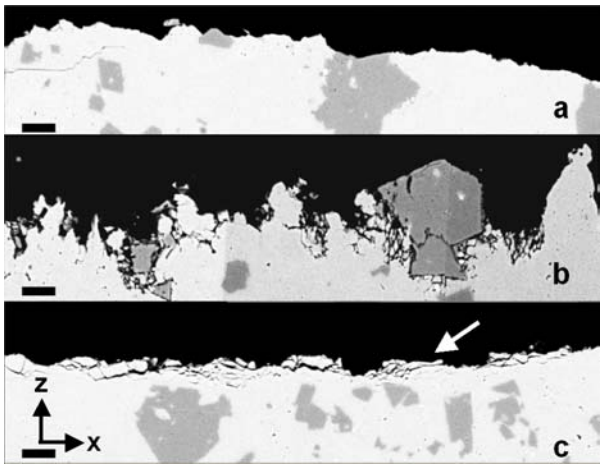

Figure 5: SEM cross-sections of the limestone hand sample. The scale bars are 30 µm. **(a)** shows the fresh limestone surface. **(b)** shows the weathered limestone surface. Note there is little material evident that is thin in the z-axis direction (perpendicular to the surface). However, pits are clearly evident. **(c)** shows the grit-blasted limestone. Thin, fractured material is evident at the surface (arrow). Note the fractured material is thin in the z-axis direction. Sample 4-12-C.

Three scales of roughness. Surface roughness that can reduce the target detectability may be present on three broad scales in geologic material. Scale 1 roughness is the gaps between individual particles or rocks in a mound (e.g., in deposits of sand, pebbles or boulders). We refer to this as the "intra-particle scale". Scale 2 is the surface at a scale that is larger than the grain, which is usually visible by eye (e.g., pitted rocks, "broad surface scale"). Scale 3 is surface roughness at the grain scale (e.g., Fig. 5, "grain scale") [*Kirkland et al*., 2002a].

In the field, the calcrete displays all three scales of surface roughness. The attenuated spectral contrast in the Figure 1 field and airborne vs. the laboratory calcrete spectra is consistent with roughness at scales not reproduced in the laboratory, which in this case were (1) gaps between individual rocks in a mound ("intra-particle scale") and (2) surface roughness much larger than the laboratory instrument spot size ("broad surface scale"). The results illustrate the typical case where the laboratory instrument mainly senses the grain scale roughness and a subset of the broad surface roughness. In contrast, the field and airborne instruments integrate over roughness at the grain scale, intra-rock scale, and the full broad surface scale.

The calcrete regional geologic unit formed and weathered in a terrestrial environment; however, the physics of spectral behavior hold true regardless of the sample origin. The effects of surface texture at multiple scales must be considered for reliable interpretations of remotely sensed data from any planetary surface.

Impact on compositional and abundance modeling. The impact of surface and volume scattering (i.e., surface texture and particle size) on compositional and abundance interpretations can be divided into three cases.

Case 1: Physical effects reduce the spectral contrast to the point that the bands are undetectable by the instrument (infrared stealthy). This includes the case when spectra measured of the same location are averaged to increase the signal-to-noise ratio, yet still do not show spectral features (e.g., "White Rock" in the *Ruff et al*. [2001] study). A more sensitive instrument may help in this situation (e.g., increased signal-to-noise ratio, use of a spectrometer rather than multi-channel radiometer). Case 1 behavior impacts compositional modeling (and potentially the resulting interpretations) when materials that are actually present are interpreted as absent, and when no minerals are detected at all.

Case 2: A cavity effect alone causes the spectral contrast to vary, but spectral features remain observable by the instrument. Case 2 behavior makes spectral contrast variations an uncertain measure of abundance. Spectral contrast variations caused by varying surface texture vs. varying abundance cannot be separated unless the variations in the target's true spectral contrast are independently known.

However, compositional modeling (e.g., linear mixture modeling) of the bands that are evident can proceed by simple scaling of the laboratory spectrum to the remotely sensed bands [*Adams et al*., 1993]. For example, the Fig. 4 fresh surface spectrum could be scaled to match the Fig. 4 weathered surface spectrum and thus correctly identify the material.

Thus Case 2 behavior increases the uncertainties in (1) mapping variations in mineral abundance and (2) compositional mixture modeling of heterogeneous materials when the different minerals have different surface textures.

Case 3: Volume absorption alters the band shape (e.g., Fig. 4 grit-blasted limestone spectrum). The simple scaling described above for Case 2 will not account for an altered band shape, and a spectral mismatch results. For example, the Fig. 4 fresh surface spectrum could not be scaled to match the Fig. 4 grit-blasted surface spectrum accurately, even though they are the same composition (same sample). *Salisbury et al*. [1991] illustrate the impact for a wide range of particulate minerals, including silicates. Thus the potential for volume scattering increases the uncertainties in compositional modeling of unknown targets (e.g., linear mixture modeling applied to data sets such as TES and THEMIS). The potential for a mismatch is particularly acute when modeling incorporates only laboratory signatures measured of large particle sizes and smooth, solid surfaces.

5. Discussion

Current state of knowledge. The dramatic reduction in spectral contrast in Figure 1 illustrates physical effects that can cause massive mineral

deposits that are present to remain undetected, even for full pixel coverage. In addition, *Salisbury et al*. [1991] illustrate changes in spectral contrast and band shape for solids vs. particulates using laboratory spectra of a wide range of minerals.

In combination, those examples illustrate physical principles of spectral behavior that apply to all geologic materials:

(1) Effects tied to surface texture and particle size can reduce the spectral band contrast to the point that a material is undetectable by a given instrument (infrared stealthy, "Case 1" behavior), including for particulates and regional outcrops of massive materials. This likely explains why some surfaces on Mars (e.g., "White Rock") have no mineral spectral bands evident in TES data. Certainly White Rock is composed of something.

(2) Materials with optically rough surfaces will be underrepresented in TES/THEMIS/Mini-TES detections. Conversely, materials that form optically smooth surfaces, including at the grain scale, will be comparatively over-represented.

(3) Roughness occurs at three broad scales, and all can reduce detectability. It is critical to recognize that roughness includes texture at the grain scale, which can be a primary variable in whether a mineral is detectable (Fig. 5).

(4) When stating a detection limit, the following information is necessary for completeness and repeatability: the proposed surface texture, the band(s) most detectable by the flight instrument, the assumed spectral contrast of the target, the minimum band depth detectable by the flight instrument at that wavelength, and the method to calculate the detection limit for the given instrument.

(5) The ability to detect a given mineral deposit scales with the instrument sensitivity. If low spectral contrast (infrared stealthy) surface mineral deposits are exposed on Mars, then identifying them may be possible using instruments that measure with higher sensitivity (e.g., higher signal-to-noise ratio, as for SEBASS) or to a limited extent by averaging pixels measured of the same spot. Fall-back measurement strategies for each flight instrument should be assessed (e.g., when to stare and average for a rover-based instrument).

(6) Observed band depth alone should not be used as a measure of abundance: surface roughness and particle size also cause strong spectral contrast variations (Figures 1–4) ("Case 2" behavior).

(7) Volume scattering can alter the band shape and cause a spectral mismatch, especially in models that use spectra only of large particle sizes or solid surfaces ("Case 3" behavior).

The listed systematic spectral complexities are not widely recognized, which has led to the assumption that TES and THEMIS have greater capabilities for mineral identification and abundance mapping than they possess. The published detectability limits have impacted interpretations of Mars' climatic and geologic history, specific deposits, and potential landing sites. Those complexities will also impact the Mini-TES.

Research needed on surface texture. TES detection limits have been stated for smooth surfaces that are hand samples or composed of large particles [*Christensen et al*., 2001]. The detection limits remain undefined for (1) rough surfaces at all scales, (2) a range of textures, (3) small particle sizes, and (4) optically rough and smooth coatings.

As a result, previous interpretations based on non-detection will need to be reconsidered based on results from systematic studies of (1) the variation in microstructure, surface texture, and coatings for materials under the formation and weathering conditions proposed for Mars, and (2) weathered and rough surfaces (e.g., Figures 1a and 1b), including remote sensing studies outside the laboratory that are subsequently validated by field work.

It is critical to initiate studies to determine the expected surface texture of proposed materials on Mars, because if a material tends to form a rougher surface on Mars, then it will be underrepresented or missed in TES/THEMIS/Mini-TES detections. Conversely, materials that form smooth surfaces, including at the grain scale, will be comparatively over-represented. Interpretations will remain incomplete until such studies occur.

Currently, the variation in surface texture between mineral classes is poorly understood, particularly for different formation and weathering pathways and at the grain scale. Inclusion of silicates will aid understanding of what conditions make them readily detected. It will also test the current assumption that all the silicate minerals present in a weathered rock surface have the same surface texture as the laboratory case that serves

as the foundation for compositional mixture modeling of TES/THEMIS data.

It is important to extend the studies past solid vs. particulate. For example, an optically smooth hematite coating matches observed TES hematite signatures [*Kirkland et al*., 2001a; *Kirkland et al*., 2003a]. On the other hand, *Christensen et al*. [2000c] argued against a hematite coating based on examination of a hand-packed hematite sample. The divergent interpretations illustrate the importance of extending textural studies past particulate vs. solid.

Field studies needed. Laboratory thermal infrared spectrometer studies of geologic materials are extensive and extend over a long history [e.g., *Lyon*, 1963; *Lyon*, 1964; *Buettner and Kern*, 1965; *Hunt*, 1965; *Aronson et al*., 1966; *Aronson et al*., 1967; *Hunt and Vincent*, 1968; *Vincent and Hunt*, 1968; *Conel*, 1969; *Hunt and Logan*, 1972; *Farmer*, 1974; *Hunt*, 1976 *Estep-Barnes*, 1977; *Salisbury et al*., 1987; *Salisbury et al*., 1991; *Salisbury and Wald*, 1992; *Lane and Christensen*, 1997; *Mustard and Hays*, 1997; *Lane and Christensen*, 1998; *Ramsey and Christensen*, 1998; *Feely and Christensen*, 1999; *Lane*, 1999; *Christensen et al*., 2000b; *Christensen et al*., 2000c; *Christensen et al*., 2001; *Wyatt et al*., 2001].

However, interpreters of remote sensing data need experience using field data that are measured similarly to the flight spectrometer (e.g., TES, Mini-TES). This recommendation was also put forth in a report developed at an open community workshop [*Kirkland et al*., 2003b]. Field studies can (1) uncover critical spectral effects not typically reproduced in laboratory studies; (2) test remote sensing interpretations against results from field research; and (3) develop tools to convey documentable interpretations and uncertainties in remote sensing data to the broader community.

However, terrestrial airborne and satellite thermal infrared studies have focused on instruments that differ fundamentally from TES. Multichannel radiometer ("multi-spectral") data sets have been used, typically that measure with four to ten bands [e.g., *Vincent et al*., 1972; *Vincent and Thomson*, 1972; *Kahle and Rowan*, 1980; *Kahle and Goetz,* 1983; *Gillespie et al*., 1984; *Abrams et al*., 1991; *Fujisada and Ono*, 1991; *King et al*., 1996; *Barnes et al*., 1998, *Hook et al*., 1999]. Multi-channel radiometers can discriminate between certain spectral types, making them productive mapping tools when combined with a field study or other information. However, they return insufficient spectral detail to uncover and study the critical aspects of spectral behavior that are illustrated here by using a spectrometer (e.g. Fig. 1b) [*Crowley and Hook*, 1996; *Kirkland et al*., 2002a]. The data illustrate that the lack of spectral detail in a multi-channel radiometer can limit the opportunity for discovery.

A literature search returned only one peer-reviewed terrestrial geologic study that uses an airborne thermal infrared spectrometer that is similar to TES, and none that have been applied to interpretations of Mars data, making the work presented here the first case.

Summary. Infrared remote sensing capabilities have been debated for over 30 years in the planetary, terrestrial, defense, and intelligence communities. If one thing is clear, it is that nature does not prepare planetary materials for an ideal, or even an easy spectroscopic experiment [*Salisbury and Hunt*, 1971]. However, infrared remote sensing is the primary method to survey planetary surface properties and composition. Mars is too large to explore thoroughly with surface investigations alone [*Salisbury and Hunt*, 1971]. In addition, rovers and landers must also remotely identify targets for rover operations and site investigations. The clear value of infrared remote sensing in planetary exploration makes an open discussion of the uncertainties imperative.

We have discussed three scientific issues of importance to planetary exploration:

(1) Volume and surface scattering (i.e., roughness and surface texture at three broad scales, and particle size) impact target detectability, compositional modeling, and abundance mapping. The physics apply to all mineral classes and are relevant to ground-based (e.g., rover), telescopic, and spacecraft infrared remote sensing of planetary surfaces.

(2) Potential misunderstandings of the uncertainties in TES and THEMIS mineral identification and mapping capabilities can impact interpretations, inferences of the geologic history and surface chemistry of Mars, and landing site selection.

(3) Studies that incorporate laboratory, field, and airborne spectrometers are needed to build experience within the community, uncover, understand, and reduce the uncertainties, and to convey them to the broader community.

Acknowledgements. We thank the Lunar and Planetary Institute (LPI) and The Aerospace Corporation (Aerospace) for supporting research into the fundamental physics behind infrared remote sensing of solid surfaces. We thank Eric Keim and John Hackwell (Aerospace) for valuable discussions and use of their unique SEBASS data, and Steven Young, Karl Westberg (Aerospace), and John Salisbury (Johns Hopkins University, *retired*) for valuable discussions. We thank three anonymous reviewers, two editors, Steven Clifford (LPI), Walter Kiefer (LPI), and Donald Burt (Arizona State University) for their thoughtful comments that improved the manuscript. We are also indebted to the years of pioneering work of the research group led by John Salisbury and Graham Hunt for their prolific contributions to founding studies of solid phase spectral behavior.

References

Abrams, M., E. Abbott, and A. Kahle, Combined use of visible, reflected infrared, and thermal infrared images for mapping Hawaiian lava flows, *J. Geophys. Res., 96*, 475–484, 1991.

Adams, J. B., M. O. Smith, and A. R. Gillespie, Imaging spectroscopy: Interpretations based on spectral mixture analysis, *Ch.7* in *Remote Geochemical Analysis: Elemental and Mineralogical Composition*, C. Pieters and P. Englert ed., Cambridge UP, 1993.

Adler, H. H. and P. F. Kerr, Infrared absorption frequency trends for anhydrous normal carbonates, *Am. Mineralogist, 48*, 124–137, 1963.

Aronson, J. R., A. G. Emslie and H. G. McLinden, Infrared spectra from fine particulate surfaces, *Science, 152*, 345–346, 1966.

Aronson, J. R., A. G. Emslie, R. V. Allen, and H. G. McLinden, Studies of the middle- and far-infrared spectra of mineral surfaces for application in remote compositional mapping of the moon and planets, *J. Geophys. Res.*, *72*, 687–703, 1967.

Bandfield, J. L. and M. D. Smith, Multiple emission angle surface–atmosphere separations of Thermal Emission Spectrometer data, *Icarus, 161*, 47–65, 2003.

Bandfield, J. L., T. D. Glotch, and P. R. Christensen, Spectroscopic Identification of Carbonates in the Martian Dust, *Lunar Planet. Sci. Conf.* [CD-ROM], *XXXIV,* abstract 1723, 2003.

Barnes, W. L., T. S. Pagano, and V. V. Salomonson, Prelaunch characteristics of the Moderate Resolution Imaging Spectroradiometer (MODIS) on EOS-AM1, *IEEE Trans. on Geoscience and Rem. Sens., 36*, 1088–1100, 1998.

Bartell, F. O., New design for blackbody simulator cavities, *SPIE Vol. 308, Contemporary Infrared Standards and Calibration*, 22–27, 1981.

Bates, R. L. and J. A. Jackson, *Dictionary of Geological Terms 3rd ed*., Doubleday, New York, 1983.

Bedford, R. E., C. K. Ma, Z. Chu, Y. Sun, and S. Chen, Emissivities of diffuse cavities. 4: Isothermal and nonisothermal cylindro-inner-cones, *Applied Optics, 24*, 2971–2980, 1985.

Blaney, D. L. and T. B. McCord, An observational search for carbonates on Mars, *J. Geophys. Res., 94*, 10159–10166, 1989.

Buettner, K. J. K. and C. D. Kern, The determination of infrared emissivities of terrestrial surfaces, *J. Geophys. Res., 70*, 1329–1337, 1965.

Carr, M. H. *Water on Mars*, 229 pp., Oxford University Press, New York, 1996.

Carr, M. H. *et al.*. *An Exobiological Strategy for Mars Exploration*, NASA SP–530, 1994.

Carr, M. H. and J. Head III, Oceans on Mars: An Assessment of the Observational Evidence and Possible Fate, *J. Geophys. Res.*, *108*, No. E5, 10.1029, 2003.

Christensen, P. R., B. M. Jakosky, H. H. Kieffer, M. C. Malin, H. Y. McSween, K. Nealson, G. Mehall, S. Silverman, and S. Ferry, The Thermal Emission Imaging System (THEMIS) instrument for the Mars 2001 Orbiter, in *Workshop on Mars 2001: Integrated Science in Preparation for Sample Return and Human Exploration*, Houston, Oct. 2-4, *LPI Contribution No.991*, 28–30, 1999.

Christensen, P. R., Mehall, N. Gorelick, S. Silverman, and the Athena Team, The Athena Miniature Thermal Emission Spectrometer (Mini-TES), in *Concepts and Approaches for Mars Exploration*, Houston, July 18–20, *LPI Contribution No.1062*, 67–68, 2000a.

Christensen, P. R., J. L. Bandfield, V. E. Hamilton, D. A. Howard, M. D. Lane, J. L. Piatek, S. W. Ruff, and W. L. Stefanov, A thermal emission spectral library of rock-forming minerals, *J. Geophys. Res*., *105*, 9735–9739, 2000b.

Christensen, P. R., J. L. Bandfield, R. N. Clark, K. S. Edgett, V. E. Hamilton, T. Hoefen, H. H. Kieffer, R. O. Kuzmin, M. D. Lane, M. C. Malin, R. V. Morris, J. C. Pearl, R. Pearson, T. L. Roush, S. W. Ruff, and M. D. Smith, Detection of crystalline hematite mineralization on Mars by the Thermal Emission Spectrometer: Evidence for near-surface water, *J. Geophys. Res*., *105*, 9632–9642, 2000c.

Christensen, P. R., and the TES team. Mars Global Surveyor Thermal Emission Spectrometer experiment: Investigation description and surface science results, *J. Geophys. Res*., *106*, 23823–23871, 2001.

Clark, B., On the non-observability of carbonates on Mars, *Fifth International Conf. on Mars, abs. 6214*, 1999.

Clark, R. N. and T. L. Roush, Reflectance spectroscopy: quantitative analysis techniques for remote sensing applications, *J. Geophys. Res., 89*, 6329–6340, 1984.

Conel, J. E. Infrared emissivities of silicates: Experimental results and a cloudy atmosphere model of spectral emission from condensed particulate mediums, *J. Geophys. Res*., *74*, 1614–1634, 1969.

Elachi, C., *Introduction to the Physics and Techniques of Remote Sensing*, Wiley&Sons, New York, 1987.

Estep-Barnes, P. A., Infrared Spectroscopy, ch.11 in *Physical Methods in Determinative Mineralogy*, ed. J. Zussman, 2nd ed., 1977.

Fabbri, M., M. Picollo, S. Porcinai, and M. Bacci, Mid-infrared fiber-optics reflectance spectroscopy: A non-invasive technique for remote analysis of painted layers. Part I: Technical set-up, *Appl. Spec*., *55*, 420–427, 2001.

Farmer, V. C. *ed*., *The Infrared Spectra of Minerals*, V. C. Mineralogical Society Press, London, 1974.

Farmer, J. D. and D. J. Des Marais, Exploring for a record of ancient Martian life. *J. Geophys. Res*., *104*, 26,977–26,995, 1999.

Feely, K. C. and P. R. Christensen, Quantitative compositional analysis using thermal emission spectroscopy: Application to igneous and metamorphic rocks, *J. Geophys. Res., 104*, 24195–24210, 1999.

Fonti, S., A. Jurewicz, A. Blanco, M. I. Blecka, and V. Orofino, Presence and detection of carbonates on the Martian surface, *J. Geophys. Res., 106*, 27815–27822, 2001.

Fraden, J. *AIP Handbook of Modern Sensors*, p.136, AIP, New York, Yew York, 1993.

Fujisada, H. and A. Ono, Overview of ASTER design concept, in *Future European and Japanese Remote-Sensing Sensors and Programs*, 1-2 April 1991, Orlando, Florida – Proceedings of the SPIE-The International Society for Optical Engineering Vol. 1490, P. Slater, Ed., Society of Photo-Optical Instrumentation Engineers, Bellingham, Washington, 244–254, 1991.

Gardner, L. R., *The Quaternary Geology of the Moapa Valley, Clark County, Nevada*, Ph.D. thesis, Pennsylvania State University, 1968.

Gardner, L. R., Origin of the Mormon Mesa caliche, Clark County, Nevada, *Geol. Soc. Am. Bull. 83*, 143–156, 1972.

Gillespie, A. R., A. B. Kahle, and F. D. Palluconi, Mapping alluvial fans in Death Valley, California, using multichannel thermal infrared images, *Geophys. Res. Lett., 11*, 1153–1156, 1984.

Ginsburg, N., W. R. Fredrickson and R. Paulson, Measurements with a spectral radiometer, *J. Optical Soc. Am*., *50*, 1176–1186, 1960.

Goetz, A. F. H., Differential infrared lunar emission spectroscopy, *J. Geophys. Res., 73*, 1455–1466, 1968.

Hackwell, J. A., D. W. Warren, R. P. Bongiovi, S. J. Hansel, T. L. Hayhurst, D. J. Mabry, M. G. Sivjee, and J. W. Skinner, LWIR/MWIR Imaging Hyperspectral Sensor for Airborne and Ground-Based Remote Sensing, *Imaging Spectrometry II, Proceedings of the International Soc. for Optical Eng*., 2819, 102–107, 1996.

Haertel, V. *Optoelectronics: Theory and Practice*, p.86, McGraw-Hill, New York, 1978.

Hapke, B., *Theory of Reflectance and Emittance Spectroscopy*, Cambridge UP, 1993.

Hanel, R. A., B. J. Conrath, D. E. Jennings, and R. E. Samuelson, *Exploration of the Solar System by Infrared Remote Sensing*, Cambridge UP, 1992.

Hecht, E., *Optics*, 2nd ed., p.110, Addison-Wesley, Reading, Massachusetts, 1987.

Hook, S. J., E. A. Abbott, C. Grove, A. B. Kahle, and F. Palluconi, Use of multispectral thermal infrared data in geological studies, Ch. 2 in *Remote Sensing for the Earth Sciences: Manual of Remote Sensing, 3rd ed. Vol. 3,* A. N. Rencz editor, 59–110, 1999.

Hovis, W. A. and W. R. Callahan, Infrared reflectance spectra of igneous rocks, tuffs, and red sandstone from 0.5–22 microns, *J. Opt. Soc. Am., 56*, 639–643, 1966.

Huang, C. K. and P. F. Kerr, Infrared study of the carbonate minerals, *Am. Mineralogist, 45*, 311–324, 1960.

Hunt, G. R., Infrared spectral emission and its application to the detection of organic matter on Mars, *J. Geophys. Res., 70*, 2351–2357, 1965.

Hunt, G. R., Infrared spectral behavior of fine particulate solids, *J. Phys. Chem., 80*, 1195–1198, 1976.

Hunt, G. R. and R. K. Vincent, The behavior of spectral features in the infrared emission from particulate surfaces of various grain sizes, *J. Geophys. Res.*, *73*, 6039–6046, 1968.

Hunt, G. R. and L. M. Logan, Variation of single particle mid-infrared emission spectrum with particle size, *Appl. Opt*., *11*, 142–147, 1972.

Judd, D. B., Terms, definitions, and symbols in reflectometry, *J. Optical Soc. Am*., *57*, 445–452, 1967.

Kahle, A. B. and L. C. Rowan, Evaluation of multispectral middle infrared aircraft images from lithologic mapping in the east Tintic Mountains, Utah, *Geology, 8*, 234–239, 1980.

Kahle, A. B. and A. F. H. Goetz, Mineralogic information from a new airborne thermal infrared multispectral scanner, *Science, 222*, 24–27, 1983.

Kahle, A. B. and R. E. Alley, Separation of temperature and emittance in remotely sensed radiance measurements, *Remote Sens. Environ., 42*, 107–111 1992.

King, M. D. and the MAS instrument team, Airborne scanning spectrometer for remote sensing of cloud,

aerosol, water vapor, and surface properties, *J. Atmospheric. and Oceanic Technology, 13*, 777–794, 1996.

Kirkland, L. E., K. C. Herr, and P. M. Adams, Searching for an improved spectral match to TES and IRIS Sinus Meridiani spectra: Coatings and cemented materials, *Eos Trans. AGU, 82*(20), *abstract*, S242, 2001a.

Kirkland, L. E., K. C. Herr, and J. W. Salisbury. Band Detection Limits in Thermal Infrared Spectra, *Appl. Opt*., *40*, 4852–4862, 2001b.

Kirkland, L. E., K. C. Herr, E. R. Keim, P. M. Adams, J. W. Salisbury, J. A. Hackwell, and A. Treiman, First Use of an Airborne Thermal Infrared Hyperspectral Scanner for Compositional Mapping, *Remote Sens. Environ.*, *80*, 447–459, 2002a.

Kirkland, L. E., K. C. Herr, P. M. Adams, J. M. McAfee, and J. W. Salisbury, Thermal infrared hyperspectral imaging from vehicle-carried instrumentation, *Proceedings of SPIE, 4816: Imaging Spectrometry VIII*, S. Shen ed., 415–425, 2002b.

Kirkland, L.E., K. C. Herr, P. M. Adams, and J. W. Salisbury, Hematite coatings match TES spectra of Sinus Meridiani, Mars, *Lunar Planet. Sci. Conf.* [CD-ROM], *XXXIV,* abstract 1944, 2003a.

Kirkland, L. E., M. Sykes, T. Farr, J. Adams, and D. Blaney, Strategies to Support Exploration of Mars' Surface, *Eos, Vol. 84, No. 16*, pp.148 and 153, 2003b.

Korb, A. R., J. W. Salisbury, and D. M. D'Aria, Thermal-infrared remote sensing and Kirchhoff's Law 2. Field measurements, *J. Geophys. Res.*, *104*, 15339–15350, 1999.

Lane, M. D. and P. R. Christensen, Thermal infrared emission spectroscopy of anhydrous carbonates, *J. Geophys. Res., 102*, 25,581–25,592, 1997.

Lane, M., R. V. Morris, and P. R. Christensen, An extensive deposit of crystalline hematite in Terra Meridiani, Mars, *Lunar Planet. Sci. Conf.* [CD-ROM] *XXX,* abstract 1469, 1999.

Lane, M. D., Midinfrared optical constants of calcite and their relationship to particle size effects in thermal emission spectra of granular calcite, *J. Geophys. Res., 104*, 14099–14108, 1999.

LaRocca, A. J. Artificial Sources, Ch.2 in *The Infrared Handbook*, Wolfe, W. & Zissis, G. ed., ERIM Press, 1978.

Le Bras, A. and S. Erard, Reflectance spectra of regolith analogs in the mid-infrared: effects of grain size, *Planet. Space Sci., 51*, 281–294, 2003.

Lyon, R. J. P., *Evaluation of Infrared Spectrophotometry for Compositional Analysis of Lunar and Planetary Soils*, NASA TN-D-1871, 1963.

Lyon, R. J. P., *Evaluation of Infrared Spectrophotometry for Compositional Analysis of Lunar and Planetary Soils*, Part 2, NASA CR-100, 1964.

McKay, C. P. and S. Nedell, Are there carbonate deposits in the Valles Marineris, Mars?, *Icarus, 73*, 142–148, 1988.

Mukhin, L. M., A. P. Koscheev, Y. P. Dikov, J. Huth, and H. Wänke, Experimental simulations of the photodecomposition of carbonates and sulphates on Mars, *Nature*, *379*, 141–143, 1996.

Mustard, J. F. and J. E. Hays, Effects of hyperfine particles on reflectance spectra from 0.3 to 25 μm, *Icarus, 125*, 145–163, 1997.

Nicodemus, F. E., Directional reflectance and emissivity of an opaque surface, *Appl. Optics*, *4*, 767–774, 1965.

Planck, M. *The Theory of Heat Radiation*, (translation by M. Masius), AIP, 1914.

Pollack, J. B., J. F. Kasting, S. M. Richardson, and K. Poliakoff, The case for a wet, warm climate on Early Mars, *Icarus*, *71*, 203–224, 1987.

Ramsey, M. S. and P. R. Christensen, Mineral abundance determination: Quantitative deconvolution of thermal emission spectral, *J. Geophys. Res., 103*, 577–596, 1998.

Roush, T. L., D. L. Blaney, and R. B. Singer, The surface composition of Mars as inferred from spectroscopic observations, Ch. 16 in *Remote Geochemical Analysis: Elemental and Mineralogical Composition*, C. Pieters and P. Englert ed., Cambridge UP, 1993.

Ruff, S. W., P. R. Christensen, R. N. Clark, H. H. Kieffer, M. C. Malin, J. L. Bandfield, B. M. Jakosky, M. D. Lane, M. T. Mellon, and M. A. Presley, Mars' "White Rock" feature lacks evidence of an aqueous origin: Results from Mars Global Surveyor, *J. Geophys. Res.*, *106*, 23921–23928, 2001.

Salisbury, J. W. and G. R. Hunt, Spectroscopic remote sensing of water-bearing minerals, Vol. 25 of AAS Science and Technology Series, *Geological Problems in Lunar and Planetary Research*, 35–52, 1971.

Salisbury, J. W., B. Hapke, and J. W. Eastes, Usefulness of weak bands in midinfrared remote sensing of particulate planetary surfaces, *J. Geophys. Res*., *92*, 702–710, 1987.

Salisbury, J. W., L. S. Walter, N. Vergo, and D. M. D'Aria, *Infrared (2.1–25 μm) Spectra of Minerals*, Johns Hopkins UP, Baltimore, 1991.

Salisbury, J. W. and A. Wald, The role of volume scattering in reducing spectral contrast of reststrahlen bands in spectra of powdered minerals, *Icarus*, *96*, 121–128, 1992.

Salisbury, J. W., Mid-infrared spectroscopy: Laboratory data, *ch.4 in Remote Geochemical Analysis: Elemental and Mineralogical Composition*, C. Pieters and P. Englert ed., Cambridge UP, 1993.

Siegel, R. and J. Howell, *Thermal Radiation Heat Transfer Vol. 1*, NASA SP-164, 1968.

Smith, M. D., J. L. Bandfield, and P. R. Christensen, Separation of atmospheric and surface spectral features in Mars Global Surveyor Thermal Emission Spectrometer (TES) studies, *J. Geophys. Res.*, *105*, 9589–9607, 2000.

Van Tassel, R. A. and J. W. Salisbury, The composition of the Martian surface, *Icarus, 3*, 264–269, 1964.

Vincent, R. K. and G. R. Hunt, Infrared reflectance from mat surfaces, *Appl. Opt*., *7*, 53–58, 1968.

Vincent, R. K., F. Thomson, and K. Watson, Recognition of exposed quartz sand and sandstone by two-channel infrared imagery, *J. Geophys. Res., 77*, 2473–2477, 1972.

Vincent, R. K. and F. Thomson, Spectral composition imaging of silicate rocks, *J. Geophys. Res.*, *77*, 2465–2472, 1972.

White, W. B., The carbonate minerals, Ch. 12 in *The Infrared Spectra of Minerals*, V. C. Farmer, *ed*., Mineralogical Society Press, London, 1974.

Williams, C. S. and O. A. Becklund, *Optics: A Short Course for Engineers*, 58–63, 1984.

Williams, C. S. Discussion of the theories of cavity-type sources of radiant energy, *J. Opt. Soc. Am.*, *51*, 564–571, 1961.

Williams, S. H. and J. R. Zimbelman, "White Rock": An eroded Martian lacustrine deposit(?), *Geology*, *22*, 107–110, 1994.

Wyatt, M. B., V. E. Hamilton, H. Y. McSween, P. R. Christensen, and L. W. Taylor, Analysis of terrestrial and Martian volcanic compositions using thermal emission spectroscopy: 1. Determination of mineralogy, chemistry, and classification strategies, *J. Geophys. Res. 106*, 14711–14732, 2001.